Craniofacial reconstruction based on skull-face models extracted from MRI datasets

M. Salas and S. Maddock

Department of Computer Science, University of Sheffield, UK

Email: {M.Salas | S.Maddock}@dcs.shef.ac.uk

Abstract

We present a method for extracting skull and face models from MRI datasets and show how the resulting dataset is used in a craniofacial reconstruction (CFR) system. Datasets for 60 individuals are used to produce a database of 3D skull-face models, which are then used to give faces to unknown skulls. In addition to the skull-face geometry, other information about the individuals is known and can be used to aid the reconstruction process. The results of the system were evaluated using different criteria providing the system with different combinations of age, gender, body build and geometric skull features. Based on a surface to surface distance metric, the real and estimated faces produced were compared using different head models from the database with a leave-one-out strategy. The reconstruction scores obtained with our CFR system were comparable in magnitude (average distance less than 2.0 mm), to other craniofacial reconstruction systems. The results suggest that it is possible to obtain acceptable face estimations using MRI based skull-face information sources in a CFR system.

1. Introduction

Craniofacial reconstruction techniques are used in forensic applications when other methods of identification cannot be applied [Evi00]. In these situations, a forensic artist using skull-face anthropometric data creates facial estimations based on her experience, the biological information deduced from the skull and other external sources of information such as *in situ* evidence. Usually, the data about the skull-face relation is based on anthropometric tables containing tissue depth measurements at a discrete set of points distributed in prominent areas of the skull and face. When manual reconstruction techniques are used, due to the subjectivity introduced by the artist and the limited information on the skull-face relation, the results are difficult to reproduce and evaluate. Computational techniques can also be used for producing face estimations. However, the results are limited when only anthropometric tables are used due to the amount and type of data available. Modern 3D scanning technologies, which are able to produce detailed data can be used to generate new information sources. We present a technique for creating accurate skull and face models from MRI data, and show the benefits of using these models in CFR.

Extracting the face layer is relatively straightforward for MRI data using the marching cubes isosurfacing technique [LC87], since only the border of the head volume needs to be identified. Extracting the skull is more difficult. Section 2 will describe previous attempts to do this and present our approach, which is based on a 3D deformation model guided by features in the MRI volume and statistical skull shape information. Section 3 will present the craniofacial reconstruction process that we have developed, based on the skull-face models extracted from the MRI datasets. Section 4 will present the results, with Section 5 presenting conclusions.

2. Skull extraction

2.1. Previous work

MRI skull segmenation has been a research topic for several years [RBH*00, DSL05, MMB06, RBH*00]. Previous work has tried to conduct this segmentation process by considering homogeneity properties of bone regions. Assuming that skull voxels possess specific attributes allowing their classification in terms of intensity, colour, texture or movement, most of the approaches provide acceptable results only in certain areas of the head. Separability assumptions of tis-

sue types are difficult to meet when presented with skull regions in MRI. The air and the skull voxels have practically no difference in intensity, colour or texture attributes. The only difference is the spatial position of each voxel relative to the global structure of the skull. Another property difficulting the skull extraction process is the high intensity variation in regions of bone where fat concentrations are found. Mathematical Morphology, a method of image analysis used for extracting image components providing a quantitative description of geometrical structures have been used for extracting the skull [DSL05, JTP01]. In some regions of the skull (e.g. the upper part) these techniques provide accepatble results but fail in the frontal area. Probabilistic approaches which have been used succesfully for classifying tissue types in medical images [CSB07, BA07] have also been used for skull segmentation with similar results in the frontal area of the skull [DSL05]. With models of parameterised distributions for each type of tissue, they try to solve the partial volume problem in order to produce adequate voxel classifications [LMVS03, LFB98, HED*97]. Deformable models based methods guided by voxel intensities are another type of technique that have been used. The works of Rifai [RBH*00], Mang [MMB06], and Ghadimi [GAMK*08] are examples of these techniques. Again, these techniques rely on separability and regularity assumptions of the materials to segment. The method proposed by Shan [SHJ*07] for segmenting the skull combines CT and MRI in a registration approach. A set of skull models generated from CT segmentations is used for segmenting skull data in MRI modalities. The main drawback of combining CT and MRI technologies is that they require a number of CT scans in order to produce the initial skull models. CT scans produce a high radiation dose that can be harmful. Also the segmentation produced is simply a collection of isolated voxels that in a second stage have to be integrated to create a skull model. Based on several deformable skull templates defined at different resolutions, Luthi et. al. combine a deformable model approach with a shape restriction term generated of training skull shapes [LLA*08]. The results of each deformed model are combined to produce a segmentation. The approach requires several skull samples to make the skull shape term robust. In contrast, our method requires a unique initial deformable model and a small set of sampled skull shapes.

2.2. Our approach

In this research, a probabilistic method to approximate a 3D skull model from an MRI volume of the head is presented. The method uses a deformable model which iteratively adjusts its shape to fit the skull embedded in a MRI volume. Shape changes in the deformable model are defined combining two elements: information provided by the MRI volume and knowledge about the 3D structure of a skull shape. The influence of these two components is modelled as a Bayesian energy formulation:

$$E(M) = E_{volume}(f, V) + \gamma E_{shape}(M) \qquad (1)$$

where E is the energy provided by the deformable model M, V is the MRI volume, f is a set of features associated with the volume V, E_{volume} is an energy function of the features and E_{shape} is the energy contribution of the shape. The term E_{volume} is defined considering a 3D Gradient Vector Flow (GVF) field acting on the volume V. A GVF for the field $v(x)$ is defined as the equilibrium solution for the vector diffusion equation [XP00]:

$$u_t = g(|\triangledown f|)\triangledown^2 u - h(|\triangledown f|)(u - \triangledown f) \qquad (2a)$$
$$u(x, 0) = \triangledown f(x) \qquad (2b)$$

The term $h(|\triangledown f|)$ will produce a smoothly varying vector field. The term $(u - \triangledown f)$ encourages a vector field u to be close to $\triangledown f$ (gradient) computed from the data. The weighting functions g and h are used to controll the influence of each term in the result. The shape term used in this research E_{shape} is defined as follows:

$$E_{shape}(s) = -\frac{1}{2}(s - \mu)^T \Sigma_\perp^{-1}(s - \mu) \qquad (3)$$

In this equation, s is a shape descriptor of model M defined by a set of control points, μ is the average of the training set and $\Sigma_\perp$ is the covariance matrix of the training set. The shape of the skull is modelled with a Gaussian distribution of control points associated with a skull model.

2.3. Alignment of Training Shapes

To conduct the statistical shape analysis of the skull it is necessary to provide a common reference system for the skull models to be compared. Taking the definition of shape given by D.G. Kendall [DM98] which states that "Shape is all the geometrical information that remains when location, scale and rotational effects are filtered out from an object", we can achieve this by means of an alignment process on the skull models. Given a set of m training vectors $\chi = \{s_i\}_{i=1..m}$ which are centered and normalised, we are interested on finding an optimal alignment for dealing with the scale and pose estimation of the shapes [DM98], [KBCL99]. An optimal alignment of two shapes s and $\hat{s}$ with respect to rotations, translation and scaling (known as full Procrustes fit [DM98]) requires the following distance to be minimsed:

$$D^2(s, \hat{s}) = \| \hat{s} - \beta s \Gamma - 1_k \gamma^T \|^2 \qquad (4)$$

where D is the distance between the two shapes, $\beta >= 0$ is a scaling factor, Γ is a rotation matrix, 1_k is a vector of ones (k x 1) vector, and γ a vector accounting for translations. Setting the corresponding derivatives to zero, the solution for the optimal parameters $\hat{\beta}$, $\hat{\gamma}$, and $\hat{\Gamma}$ are the following expressions [KBCL99], [Sma96]:

$$\hat{\gamma} = 0 \qquad (5)$$
$$\hat{\Gamma} = UV^T \qquad (6)$$

The rotation term $\hat{\Gamma}$ is defined in terms of the matrices U and V derived from a single value decomposition of the matrix product $\frac{\hat{s}^T s}{\|s\|\|\hat{s}\|}$ as follows:

$$\frac{\hat{s}^T s}{\|s\|\|\hat{s}\|} = V\Lambda U^T \qquad (7)$$

It can be shown that the best rotation estimator $\hat{\beta}$ can be obtained by the following ratio [DM98]:

$$\hat{\beta} = \frac{trace(\hat{s}^T s \hat{\Gamma})}{trace(s^T s)} \qquad (8)$$

and finally, the expression defining the best alignment for the shape $\hat{s}$ is:

$$\hat{s} = \hat{\beta} s_c \hat{\Gamma} + 1_k \hat{\gamma}^T + \sqrt{D^2(s_c, \hat{s})} \qquad (9)$$

where s_c is the centered version of shape s. The energy can be minimised by applying the chain rule on the gradient descent equation:

$$\frac{ds}{dt} = -\frac{dE_{shape}(s)}{ds} = -\frac{dE_{shape}(\hat{s})}{d\hat{s}} \cdot \frac{d\hat{s}}{ds_c} \cdot \frac{ds_c}{ds} \qquad (10)$$

with:

$$\frac{dE_{shape}(\hat{s})}{d\hat{s}} = (\Sigma_{\perp}^{-1}(s - \mu))^T \qquad (11)$$

$$\frac{ds_c}{ds} = (I_{3n} - \frac{1}{n}\Gamma) \qquad (12)$$

$$\frac{d\hat{s}}{ds_c} = \frac{d(\hat{\beta} s_c \hat{\Gamma} + 1_k \hat{\gamma}^T + \sqrt{D^2(s_c, \hat{s})})}{ds_c} \qquad (13)$$

The terms D, $\hat{\gamma}$, $\hat{\Gamma}$, and $\hat{\beta}$ in equation 13 are all functions of the aligned shape $\hat{s}$ using the results of equations 4-8.

2.4. Deformable Model Algorithm

The algorithm to control the skull template evolution is shown in figure 2. It deforms the skull template to find a skull model that best fits the information provided by a noisy skull volume created in a pre-processing stage. The pre-processing stage receives as input the MRI volume and generates as output a nosiy volume containing a skull approximation and a vector field associated to this approximation. The initial approximation is generated by a semi-automatic region growing process [LJZ03] applied the MRI dataset [SM09]. Used as an initial guess, the noisy skull contains information about approximate proportions of the skull, position and orientation. This information that is used to reduce the search space of the solution (see figure 1). The deformation is conducted by changing the positions of a set of control points defined in the deformable model according to the volume features and the shape restrictions. The stop condition used is a fixed number of iterations.

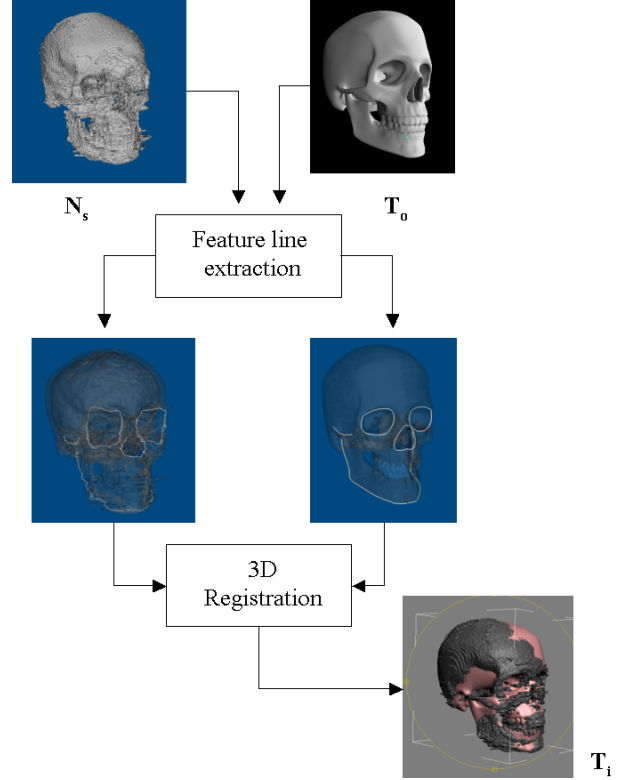At each iteration, the deformable model control points are

Figure 1: *Skull Template initialisation. A noisy skull approximation N_s is used to initialise the skull template model T_o by means of a registration step using a robust point match algorithm [CR00]*

moved towards the direction of the most probable skull configuration. The displacement of the control points is stored in 1-dimensional vectors d_1, d_2 and d_3. Vectors d_1 and d_2 accounts for changes when volume features are taken into account. d_1 has values when the deformable model is near to the noisy skull model, and it is zero when it is far from the noisy skull. d_2 stores the contribution of the Gradient Vector Flow when a control point is far from the noisy volume. Vector d_3 stores displacements originated by the shape term. The deformation function used to update the positions of the control points is based on a Radial basis function with a Thin-Plate-Spline base [CBC*01]:

$$f_k(\mathbf{x}) = p_m(\mathbf{x}) + \sum_{i=1}^{n} \alpha_i \phi_i(\|\mathbf{x} - \mathbf{x}_i\|) \qquad (14)$$

The value of the function ϕ_i depends only on the distance of the point $\mathbf{x}$ to each of the control points $\mathbf{x}_i$ (The $\mathbf{x}_i$ points are called centers). The weights of the basis functions α_i are found by placing the centres back into $f_k(\mathbf{x})$ and solving the resulting set of linear equations. The polynomial term p_m is included to allow a certain degree of polynomial precision.

```
Algorithm 1 Template Deformation
Require: Skull template properly initialised
  while (stop condition not meet) do
    Variable initialisation :
    i = d_j(x_i) = d_j(y_i) = d_j(z_i) ← 0;
    {(i,j)| 1 ≤ j ≤ 3; 0 ≤ i ≤ Number of Control Points}
    for each control point i do
      calculate intersection of the ray from CP_i (at the skull template)
      to the noisy volume in its normal direction within a range
      if (intersection exists) then
        calculate d_1(x_i), d_1(y_i), d_1(z_i) in direction of the intersecting point
        set: d_2(x_i) = d_2(y_i) = d_2(z_i) ← 0
      else
        set: d_1(x_i) = d_1(y_i) = d_1(z_i) ← 0
        calculate d_2(x_i), d_2(y_i), d_2(z_i) from the GVF direction
      end if
    end for
    Set d_3(x_i), d_3(y_i), d_3(z_i) ← 0
    Calculate Shape energy vector d_3
    Deform the model using RBF-TPS using CP_i + d_3
    Evaluate the stop condition
  end while
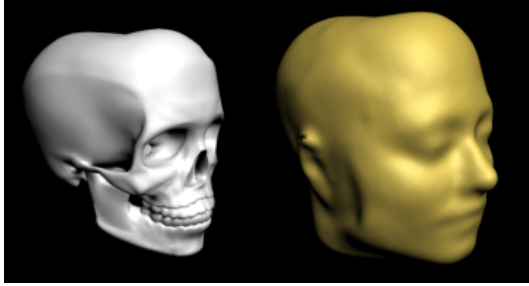```

**Figure 2:** *Template deformation algorithm.*



**Figure 3:** *The resulting surface models for the skull and face of the first individual of the database.*

The MRI dataset used in this work was created at the University of Sheffield (footnote giving details of who created the data and when). It consists of a set of scans of the head and neck of 60 subjects, and their corresponding biographical information: age, sex, ancestral affiliation (ethnicity). Additionally, information of whether the individuals relatives were also volunteering was also recorded. Each volume contains 200 gray-scaled 256 x 256 pixel sagittal images. The format of each image is 16 bit per pixel raw data with information of approximately the aorta level and up.

The algorithms described in the previous sections are used to segment this data. Figure 3 shows an example of the skull and face models generated with the extraction process. Using our extraction algorithm, a database of 60 skull-face models were generated and the 40 best models were used in the CFR system described in the next section.

## 3. Craniofacial Reconstruction System

The craniofacial reconstruction system consists of three main elements: Skull Examination, Template Construction and Face Construction. In the first stage, an input skull is analysed and a set of main features extracted. Combining these features with information about the skull-face relationship, and a spatial deformable technique, this system creates possible face estimations for the input skull. The anthropometric information is provided by the database of head models presented in section 2. The reconstruction technique is based on a template deformation approach. A head template (skull-face pair) is created by combining several heads models from the database. These models are selected with similar features to the unknown subject. The age, sex, body constitution, PCA coefficients, and geometric properties of the unknown skull are used as selection conditions. The head template is deformed to fit the unknown skull to produce face estimation. The deformation approach used is based on a Radial basis function approach with a thin plate spline base (see equation 14). A set of head models is chosen from the database considering matching criteria in terms of the unknown skull features. The use of spatial deformation allows the facial tissues (skull, muscle, etc.) to be dealt with as a single component, freeing the procedure from the problem of placing and interpreting anthropometric landmarks associated with soft tissue depth tables [MC96, VVMN00]. Facial soft tissues should change in response to the changes in the skull, and therefore the face is not merely a mask depending on a small number of soft tissue depth points, as is the case, for example, in [CVG*06]. The $k$ reference head (skull-face) models whose facial models are $F_r^i$ ($i = 1 \dots k$), are combined for producing a face estimation are contained in the set $H_b$:

$$\mathbf{H}_b = \{\mathbf{H}_r^1, \mathbf{H}_r^2 \dots \mathbf{H}_r^k\} = \{\{S_r^1, F_r^1\},$$
$$\{S_r^2, F_r^2\}, \dots \{S_r^k, F_r^k\}\} \quad (15)$$

For example, if the criterion is the minimum procrustes distance $d$ between the skull shapes [DM98], the set $\mathbf{H}_b$ of selected head models is defined as:

$$\mathbf{H}_b = \{\{S_r^i, F_r^i\} \mid i \in \{j \mid d(S_r^j, S_u)$$
$$< \varepsilon, j \in \{1 \dots n\}\}\} \quad (16)$$

where $n$ is the number of elements of the database, $S_r^j$ is a reference skull model of the $j^{th}$ database entry, and $\|\mathbf{H}_b\| = k$ for some threshold value $\varepsilon$ accounting for a limit for the difference in procrustes distance $d$ between models $S_r^j$ and $S_u$. Using a leave-one-out strategy [VCL*06], a skull $S_u \in H_u$ will simulate the skull whose face will be reconstructed and its skin layer $F_u$ will then be used to evaluate the results.

The process of face estimation is shown schematically in figure 4. In this stage, a deformation function $f$ will be calculated between $S_u$ and each of the reference skulls $S_r^j \in \mathbf{H}_b$
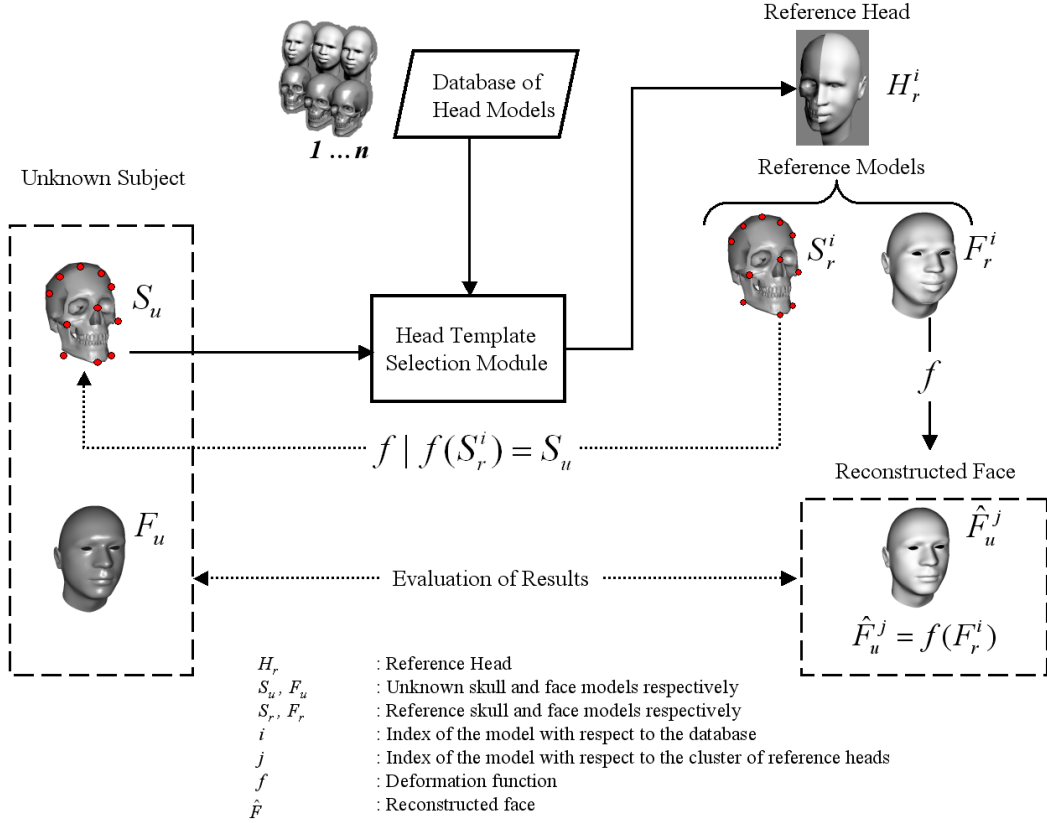
**Figure 4:** *The template selection process.*

:

$$f_j(S_r^j) = S_u \qquad (17)$$

This mapping function $f_j$ will be used to estimate a deformed face $\hat{F}_u^j$ for each of the $j$ reference models, by applying this function to the corresponding reference face $F_r^j$ as follows:

$$\hat{F}_u^j = f_j(F_r^j) \qquad (18)$$

The resulting reconstructed face $\hat{F}_u$ is then the average of the $\hat{F}_u^j$ elements:

$$\hat{F}_u = \sum_{j=1}^{k} \frac{\hat{F}_u^j}{k} \qquad (19)$$

The functions $f_j$ are based on the Radial Basis Function deformation approach [CBC*01]. The set of matching control points between the source and target models are obtained directly from the realtion between the vertices of both models (they share a common vertices structure because were originated with the skull template deformations scheme presented in section 2.4).

## 4. Results

The results of the CFR system are obtained by means of a comparison between the reconstructed face and the real face surface evaluated by using a surface to surface metric ( The average difference between both surfaces). The system was tested with 27 different combination of biological and geometrical features. Table 1 shows the criteria used for generating the craniofacial reconstructions. Negated attributes mean that different features were used to select models from the database (e.g. $\overline{Sex}$ means that the models used were of the opposite genre to the sex of the unknown skull). Negated criteria were included to quantify the impact of choosing the wrong features in the CFR system and to corroborate that positive criteria give better reconstructionn results that negative criteria. Figure 5 shows the skull 18 of the UOS dataset. Figure 6 shows 6 facial reconstructions for the skull of subject 18 of the UOS dataset. In this case, the third row shows the best face reconstruction of the group (i.e. the one with lowest average distance between surfaces) and it was obtained using models of individuals with similar age as the unknown skull $t_2$). Figures 7 and 8 show the best reconstruction generated. In the graph shown in figure 9 the aver-
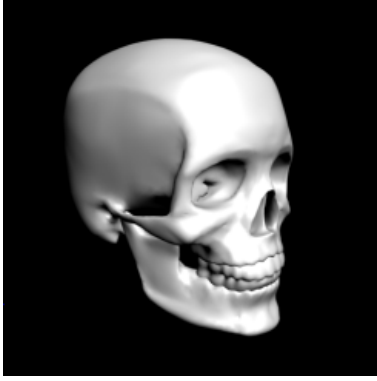
**Figure 5:** *Skull model 18 of the UOS dataset.*



age distances fom the reconstructed faces sorted by criteria used are shown. Criteria $t_0$ to $t_{14}$ show that, when adding information to the CFR system about the unknown skull, the CFR system implemented give results with less than 2.0 mm with respect to the real face. Using negative criteria, the average error was not greater than 2.5mm. An in general, as expected, positive criteria produced better results that negative criteria.

Using a leave-one-out strategy, 850 facial reconstructions were generated using different criteria based on feature matching using the sex, age, body build and geometric features of the input skull. The results obtained were comparable to other techniques using evaluation criteria based on surface to surface distance metrics obtaining average distances of less than 2.0 mm.

## 5. Conclusions

We have presented a novel approach to extracting skulls from MRI datasets, based on a probabilistic approach for guiding a 3D deformable template evolution. By incorporating shape knowledge of the skull, our approach is able to cope with uncertainty problems in regions where it is difficult to establish skull boundaries. This property is useful to overcome the strong homogeneity restrictions exposed in the methods presented in section 2.1 (most of them based only in one intensity criteria to separate skull elements).

The extraction process, in conjunction wth the use of the marching cubes algorithm [LC87] for face extraction from the MRI dataset, has been used to create a database of skull-face models for use in a craniofacial reconstruction (CFR) system. The CFR results obtained are comparable to other CFR approaches, and offer the advantage of more consistent reconstructions, with each stage being easier to control and evaluate, removing the subjectivity of artist-driven approaches. In addition, since MRI datasets can be readily obtained, the database could be easily extended. M.Salas ac-
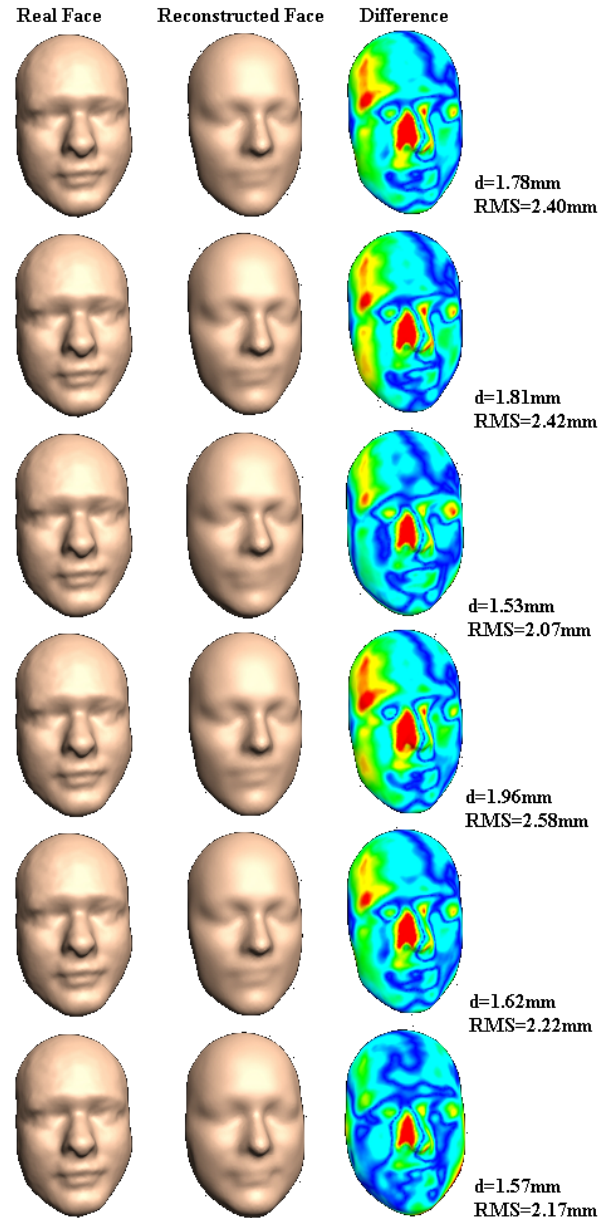
**Figure 6:** *An example of five results of the CFR system for the skull of the subject 18 of the UOS dataset. Each row represents a criteria for the reconstruction (t0-t5)*

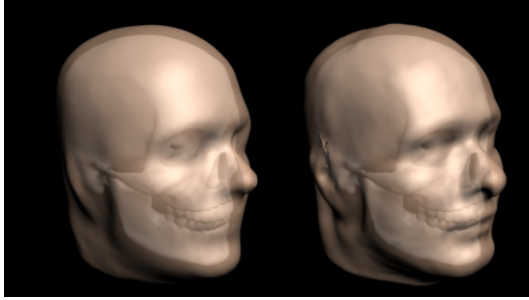**Figure 7:** *An example of the best reconstruction for skull model 18 of the UOS dataset. The figure shows the reconstructed face on the base skull (left) and the real head model of the skull (right). The best reconstruction score was obtained applying criterion t6 based on sex and age.*



**Figure 8:** *Facial surface reconstructed of the example in figure 7. Again, the reconstructed face (left) and original face (right). The results corresponds to criterion t6 (Sex & Age) with $\overline{d} = 1.42$ mm and RMS $= 1.98$ mm.*
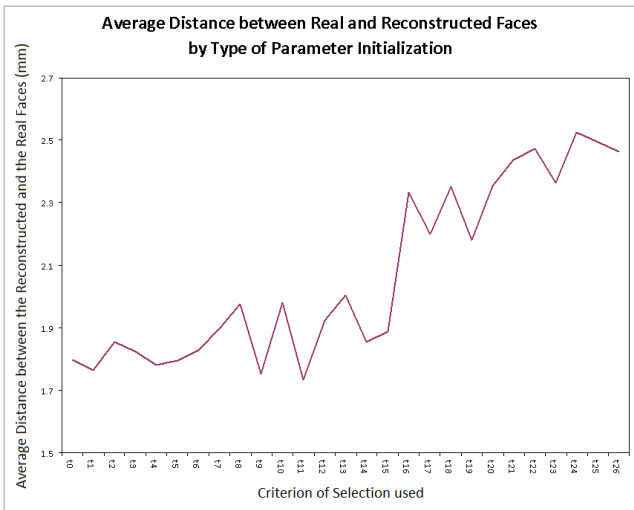


**Figure 9:** *Average distances of reconstruction for criteria presented in table 1*

| Test | Feature criteria |
|---|---|
| $t_0$ | All the database (the universal set) |
| $t_1$ | *Sex* |
| $t_2$ | *Age* band |
| $t_3$ | *PCA* band |
| $t_4$ | *Proc* distance |
| $t_5$ | *BMI* band |
| $t_6$ | *Sex & Age* |
| $t_7$ | *Sex & Age & PCA* |
| $t_8$ | *Sex & Age & Proc* |
| $t_9$ | *Sex & Age & BMI* |
| $t_{10}$ | *Sex & Age & PCA & BMI* |
| $t_{11}$ | *Sex & Age & Proc & BMI* |
| $t_{12}$ | $\overline{Sex}$ |
| $t_{13}$ | $\overline{Age}$ |
| $t_{14}$ | $\overline{PCA}$ |
| $t_{15}$ | $\overline{Proc}$ |
| $t_{16}$ | $\overline{BMI}$ |
| $t_{17}$ | $\overline{Sex}$ & $\overline{Age}$ |
| $t_{18}$ | $\overline{Sex}$ & $\overline{Age}$ & PCA |
| $t_{19}$ | $\overline{Sex}$ & $\overline{Age}$ & Proc |
| $t_{20}$ | $\overline{Sex}$ & $\overline{Age}$ & $\overline{PCA}$ |
| $t_{21}$ | $\overline{Sex}$ & $\overline{Age}$ & $\overline{Proc}$ |
| $t_{22}$ | $\overline{Sex}$ & $\overline{Age}$ & $\overline{BMI}$ |
| $t_{23}$ | $\overline{Sex}$ & $\overline{Age}$ & PCA & $\overline{BMI}$ |
| $t_{24}$ | $\overline{Sex}$ & $\overline{Age}$ & Proc & $\overline{BMI}$ |
| $t_{25}$ | $\overline{Sex}$ & $\overline{Age}$ & $\overline{PCA}$ & $\overline{BMI}$ |
| $t_{26}$ | $\overline{Sex}$ & $\overline{Age}$ & $\overline{Proc}$ & $\overline{BMI}$ |

**Table 1:** *Criteria used for the facial reconstructions.*

### References

[BA07]  BULU H., ALPKOCAK A.: Comparison of 3d segmentation algorithms for medical imaging. In *Computer-Based Medical Systems, 2007. CBMS '07. Twentieth IEEE*

*International Symposium on Computer-Based Medical Systems* (June 2007), pp. 269–274.

[CBC*01] CARR J., BEATSON R., CHERRIE J., FRIGHT T. M. W., McCALLUM B., EVANS T.: Reconstruction and representation of 3D objects with radial basis functions. In *Proceedings of ACM SIGGRAPH 2001* (2001), pp. 67–76.

[CR00] CHUI H., RANGARAJAN A.: A New Algorithm for Non-Rigid Point Matching. In *Proceedings of CVPR* (June 2000), vol. 2, pp. 40–51.

[CSB07] CLAYDEN J., STORKEY A., BASTIN M.: A probabilistic model-based approach to consistent white matter tract segmentation. *Medical Imaging 26*, 11 (November 2007), 1555–1561.

[CVG*06] CLAES P., VANDERMEULEN D., GREEF S. D., WILLEMS G., SUETENS P.: Craniofacial reconstruction using a combined statistical model of face shape and soft tissue depths: Methodology and validation. *Forensic Science International 159 (Suppl1)* (2006), 147–158.

[DM98] DRYDEN I., MARDIA K.: *Statistical Shape Analysis*. John Wiley, July 1998.

[DSL05] DOGDAS B., SHATTUCK D., LEAHY R.: *Human Brain Mapping*, vol. 26-4. Wiley-Liss, 2005, ch. Segmentation of skull and scalp in 3-D human MRI using mathematical morphology, pp. 273–285.

[Evi00] EVISON M.: Modeling Age, Obesity, and Etnicity in a Computerized 3-D Facial Reconstruction. In *9th Biennial Meeting of the International Association for Craniofacial Identificaction* (FBI, Washington DC, July 2000).

[GAMK*08] GHADIMI S., ABRISHAMI-MOGHADDAM H., KAZEMI K., GREBE R., GOUNDRY-JOUET C., WALLOIS F.: Segmentation of scalp and skull in neonatal MR images using probabilistic atlas and level set method. *Engineering in Medicine and Biology Society, 2008. EMBS 2008. 30th Annual International Conference of the IEEE* (Aug 2008), 3060–3063.

[HED*97] HEINOEN T., ESKOLA H., DASTIDAR P., LAARNE P., MALMIVUO J.: Segmentation of T1 MR scans for reconstruction of resistive head models. *Computer Methods and Programs in Biomedicine 54* (1997), 173–181.

[JTP01] JERE A., TASIC J., PERMUS F.: Izlocanje lobanje iz mr slik:segmentation of the skull in MRI volumes, October 2001. University of Ljubljana, Slovenia.

[KBCL99] KENDALL D., BARDEN D., CARNE T., LE H.: *Shape and Shape Theory*. John Wiley and Sons, 1999.

[LC87] LORENSEN W., CLINE H.: Marching Cubes: a high resolution 3D surface reconstruction algorithm. In *Computer Graphics* (1987), vol. 21-4, Proceedings of SIGGRAPH, pp. 163–169.

[LFB98] LAIDLAW D., FLEISCHER K., BARR A.: Partial-volume bayesian classification of material mixtures in mr volume data using voxel histograms. *IEEE Transactions on Medical Imaging 17* (1998).

[LJZ03] LU Y., JIANG T., ZANG Y.: Region growing method for the analysis of functional MRI data. *NeuroImage 20* (2003), 455–465.

[LLA*08] LÜTHI M., LERCH A., ALBRECHT T., KROL Z., VETTER T.: A hierarchical multi-resolution approach for model-based skull-segmentation in mri volumes. *Conference Proceedings 3D-Physiological Human* (December 2008).

[LMVS03] LEEMPUT K., MAES F., VANDERMEULEN D., SUETENS P.: A Unifying Framework for Partial Volume Segmentation of Brain MR Images. *IEEE Transactions on Medical Imaging 22*, 1 (2003), 105–119.

[MC96] MICHAEL S., CHEN M.: The 3D Reconstruction of Facial Features Using Volume Distortion. In *Proceedings 14th Eurographics UK Conference* (March 1996), pp. 297–305.

[MMB06] MANG A., MÜLLER J., BUZUG T. M.: A multi-modality computer-aided framework towards postmortem identification. *Journal of Computing and Information Technology (CIT) 14*, 1 (2006), 7–19.

[RBH*00] RIFAI H., BLOCH I., HUTCHINSON S., J.W., GARNERO L.: Segmentation of the skull in mri volumes using deformable model and taking the partial volume effect into account. *Medical Image Analysis 4*, 3 (2000), 219 – 233.

[SHJ*07] SHAN Z., HUA C., JI Q., PARRA C., YING X., KRASIN M., MERCHANT T., KUN L., REDDICK W.: A Knowledge-guided Active Model of Skull Segmentation on T1-weighted MR images. In *SPIE Medical Imaging* (March 2007), vol. 6512.

[SM09] SALAS M., MADDOCK S.: *A 3D Skull Segmentation Method Based on Deformable Models*. Tech. Rep. CS-09-10, University of Sheffield, 2009.

[Sma96] SMALL G.: *The Statistical Theory of Shape*. Springer Series in Statistics, 1996.

[VCL*06] VANDERMEULEN D., CLAES P., LOECKX D., DE GREEF S., WILLEMS G., SUETENS P.: Computerized craniofacial reconstruction using ct-derived implicit surface representations. *Forensic Science International 259 (Suppl)* (2006), 164–174.

[VVMN00] VANEZIS P., VANEZIS M., McCOMBE G., NIBLETT T.: Facial reconstruction using 3-D computer graphics. *Forensic Science International 108*, 2 (February 2000), 81–95.

[XP00] XU C., PRINCE J.: *Handbook of Medical Imaging*. Academic Press, September 2000.